ARTICLE NO. 79-0351R

Some Features of the Unsteady Pressure Field in Transonic Airfoil Buffeting

Frederick W. Roos*
McDonnell Douglas Corporation, St. Louis, Mo.

Comparisons are made between the unsteady transonic flowfields of two airfoils: a Whitcomb supercritical airfoil, and a conventional NACA 0012 section. Wind tunnel experiments on these airfoils included penetration into buffeting as a result of high c_l and/or high M_∞. Fluctuating surface pressure, lift, and shock location were measured on both airfoils. Two-point pressure cross-correlations were used to determine coherence and propagation direction of pressure fluctuation patterns on the upper surface of each airfoil. Between the upper-surface shock and the trailing edge (a region with intense pressure fluctuations), pressure disturbances propagated upstream in attached flow, but traveled downstream when extensive separation existed. In the latter case, convection velocities were found to be frequency dependent. Another cross-correlation, relating surface-pressure fluctuations to unsteady lift, was employed to establish which regions of the pressure fields were of primary importance in producing buffeting forces. While many of the principal features of the pressure/lift cross-correlations were common to both airfoils, some specific differences were found. For example, the supercritical airfoil exhibited less periodicity in its cross-correlation. This result was attributed to the flat-topped, aft-cambered shape of the supercritical airfoil section, which reduced the coupling between shock oscillations and lift fluctuations.

Nomenclature

C_p = pressure coefficient $= (p - p_\infty)/q_\infty$
C_p^* = pressure coefficient for locally sonic flow
$C_{p,te}$ = pressure coefficient at trailing edge
c = airfoil chord, m
c_l = section lift coefficient $= L/q_\infty c$
c_m' = unsteady bending moment coefficient $= m_b'/M_b$
D = drag force per unit span, N/m
f = frequency, Hz
f^* = dimensionless frequency $= fc/U_\infty$
L = lift force per unit span, N/m
M = Mach number
M_b = mean spanwise bending moment at midspan, m·N
m_b = fluctuating spanwise bending moment at midspan, m·N
p = static pressure, Pa
q = dynamic pressure $= \rho U^2/2$
$R(x,\tau)$ = autocorrelation coefficient of unsteady variable $x(t)$, Eq. (2)
$R(x,y,\tau)$ = cross-correlation coefficient relating unsteady variables $x(t)$ and $y(t)$, Eq. (3)
Re_c = Reynolds number $= U_\infty c/\nu_\infty$
U = streamwise flow speed, m/s
U_c = pressure fluctuation convection speed, m/s
w_w = unsteady downwash velocity at upper edge of wake near trailing edge, m/s
x = chordwise distance, m
x_s = chordwise displacement of shock, m
ν = kinematic viscosity, m^2/s
ρ = density, kg/m^3
τ = cross-correlation time delay, s
$(\ )'$ = root-mean-square value of unsteady component of variable
$(\ )_\infty$ = freestream value

Presented as Paper 79-0351 at the AIAA 17th Aerospace Sciences Meeting, New Orleans, La., Jan. 15-17, 1979; submitted Feb. 16, 1979; revision received March 5, 1980.

Index categories: Nonsteady Aerodynamics; Transonic Flow.

*Scientist, McDonnell Douglas Research Laboratories. Member AIAA.

Introduction

TRANSONIC buffeting limits the maneuverability of combat aircraft, and consequently remains the subject of continuing study.[1,2] Because of the highly complex nature of this challenging problem, involving the interaction between an unsteady, separated, three-dimensional, transonic flow and a multi-component, three-dimensional structure that is vibrating in several modes, theoretical prediction of buffeting intensity will remain an impossibility for a long time to come. Although rapid progress is currently being made in computational fluid dynamics, the calculation of even the two-dimensional flowfield of a rigid airfoil in transonic buffeting has yet to be accomplished. On the experimental side, attempts to use wind-tunnel measurements of surface-pressure fluctuations to predict flight buffet loads have proven to be very difficult.[3,4] Sophisticated models of transonic buffeting flows must be developed before buffeting of aircraft, or even two-dimensional airfoils, can be predicted correctly by either numerical or semiempirical methods. Definition of the necessary flow models depends upon the experimental determination of the significant details of transonic buffeting.

McDonnell Douglas Research Laboratories (MDRL) has been conducting an investigation of transonic airfoil aerodynamics in cooperation with the Douglas Aircraft Company (DAC) and the NASA Ames Research Center (ARC). One element of this program has been research into the unsteady aerodynamics responsible for buffeting. An initial series of experiments dealt exclusively with a Whitcomb-type supercritical airfoil.[5,6] Within the ranges of c_l and M_∞ studied, regions of intense pressure fluctuations were identified, variations of fluctuating pressure power spectra with local flow conditions were determined, and spanwise and chordwise coherences of pressure fluctuations and wake downwash velocity oscillations were established.

Further transonic airfoil buffeting experiments were performed recently. These new experiments covered greater c_l and M_∞ ranges for the Whitcomb-type supercritical airfoil, including penetration into heavy buffeting. In addition, a comparable set of tests was performed on the conventional NACA 0012 airfoil section to provide a hitherto unavailable set of unsteady-flow data for comparison with the supercritical airfoil results. New instrumentation provided lift fluctuation and shock oscillation measurements.

The objective of these experiments was to clarify and define the unsteady pressure field acting on the airfoils as each airfoil developed buffeting through increasing c_l and/or M_∞. Cross correlation of unsteady variables was used to determine the coherence, spatial and temporal scales, and propagation directions and speeds of unsteady pressure disturbances in the flow.

Equipment and Procedures

The experiments were conducted in the NASA Ames Two-by-Two-Ft Transonic Wind Tunnel, a continuous-flow facility that has been modified for two-dimensional testing. The 15.24-cm chord airfoil models spanned the 61-cm wide test section and were supported by rotatable windows that provided angle-of-attack variation. Figure 1 illustrates the test equipment installation.

Two airfoils were tested in this series of experiments. The supercritical section was identical to Whitcomb's original 11% thick single-element supercritical airfoil,[7] except that the model tested was modified to have a 1% thick trailing edge to permit installation of static and dynamic pressure instrumentation in the trailing edge region. The conventional airfoil tested was the NACA 0012 section.

Located at midspan on each airfoil was a chordwise row of static pressure orifices. High-frequency-response, semiconductor strain-gage pressure transducers were installed adjacent to the pressure taps on both upper and lower surfaces of the airfoils. Signal conditioning equipment for these transducers included an analog summing circuit that approximated the instantaneous lift force. The supercritical airfoil model also contained a strain-gage bridge circuit for sensing spanwise bending vibrations.

Additional instrumentation included a dynamic-response pressure probe for monitoring background disturbances in the test section, and a sting-mounted probe traversing unit. The traversing rig was capable of movements in the streamwise and vertical directions, and was used to position two probes in the airfoil flowfield simultaneously. One of these probes was a two-sensor, X-configuration, hot-film anemometer probe, used to sense downwash fluctuations near the airfoil trailing edge. The other was a newly-developed shock-position-sensing probe,[8] employed to monitor oscillations of the upper-surface shock that stood on the airfoil in transonic flow. Probe operation is similar to an anemometer probe in connection with a standard constant-temperature anemometer unit.

Dynamic data were recorded on FM tape during the wind tunnel tests. Subsequent digital data analysis followed standard statistical procedures.[9] Intensities, or root-mean-square levels, of fluctuating variables were evaluated, and auto- and cross-correlations were computed. Power spectra were generated by Fourier transformation of autocorrelation functions. In terms of arbitrary fluctuating variables $x(t)$ and $y(t)$, the various statistical quantities were defined as follows:

Intensity

$$x' = \left[\lim_{T\to\infty} \frac{1}{T}\int_0^T x^2(t)\,dt\right]^{1/2} \tag{1}$$

Autocorrelation coefficient

$$R(x,\tau) = \frac{1}{(x')^2}\lim_{T\to\infty}\frac{1}{T}\int_0^T x(t)x(t+\tau)\,dt \tag{2}$$

Cross-correlation coefficient

$$R(x,y,\tau) = \frac{1}{x'y'}\lim_{T\to\infty}\frac{1}{T}\int_0^T x(t)y(t+\tau)\,dt \tag{3}$$

Additional details concerning the experimental setup and the data reduction procedures are given in Ref. 10.

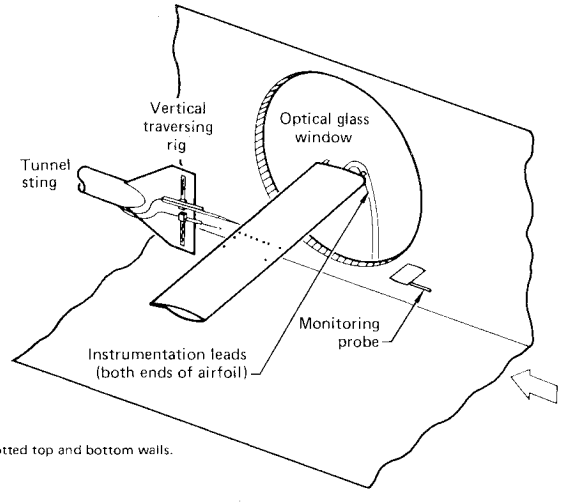

Fig. 1 Experimental arrangement for two-dimensional transonic airfoil buffeting studies.

Results and Discussion

Each airfoil was tested over a range of M_∞ and c_l values around a baseline condition that represented a typical airfoil cruise condition. For the supercritical airfoil, the baseline condition was $M_\infty = 0.82$, $c_l = 0.53$; the corresponding condition for the 0012 section was $M_\infty = 0.68$, $c_l = 0.42$. Holding either M_∞ or c_l fixed, the other variable was increased until the airfoil passed through the onset of flow separation effects and into heavy buffeting.

Airfoil Pressure Distributions

Figures 2 and 3 show how the C_p distribution for the supercritical airfoil evolved with increasing c_l and M_∞, respectively. In all cases, the upper-surface boundary layer was tripped by a transition strip located at 35% chord. Both sets of pressure distributions show clearly the characteristic aft loading of this airfoil. Also evident is the pronounced rearward shift of the shock as either c_l or M_∞ is increased. In both cases, this trend is reversed upon the appearance of flow separation, which is always of the trailing-edge type on this supercritical airfoil. The $c_l = 0.91$ curve in Fig. 2 represents a case of heavy buffeting, with separation occurring at the foot of the shock and extending beyond the trailing edge. On the other hand, Fig. 3 reveals that the highest Mach number studied, $M_\infty = 0.90$, was insufficient to produce significant buffeting, despite penetration well beyond the drag rise, which occurred at $M_\infty \approx 0.81$ at this c_l level.[6] Flow separation and trailing edge C_p divergence are clearly present at $M_\infty = 0.87$, but the shock pressure rise remains localized at $M_\infty = 0.90$, indicating the absence of buffeting fluctuations even though the separation occurs near the shock.

The variation of the pressure distribution on the conventional NACA 0012 airfoil as M_∞ increased at constant c_l is shown in Fig. 4. This section carries essentially all its loading forward; the only significant loading of the trailing-edge region occurs at the highest Mach number ($M_\infty = 0.80$), for which separation extends from the shock to the trailing edge. On this airfoil, separation first appears as a bubble at the base of the shock ($M_\infty = 0.74$). This bubble grows toward the trailing edge ($M_\infty = 0.77$) until the flow becomes fully separated and heavy buffeting results. The chordwise shifting of the shock is similar to, but less extensive than, the shock movement on the supercritical airfoil. Development of the conventional airfoil C_p distribution with increasing c_l at constant M_∞ is similar, particularly in the manner in which

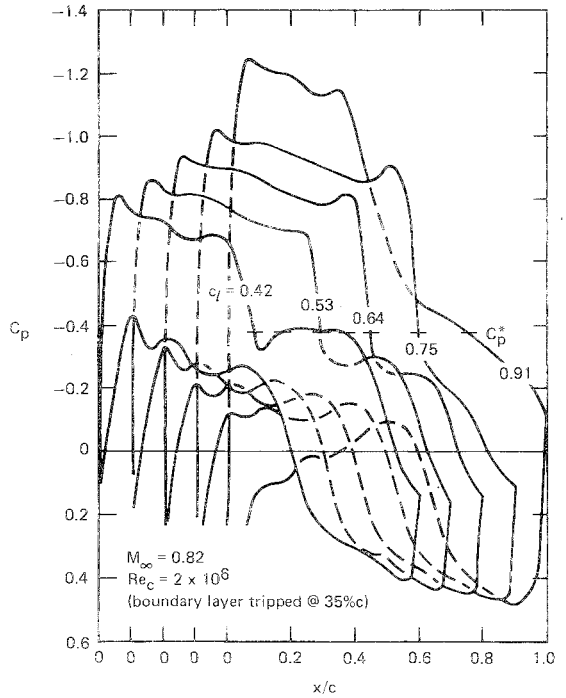

Fig. 2 Evolution with increasing lift of pressure distribution on supercritical airfoil.

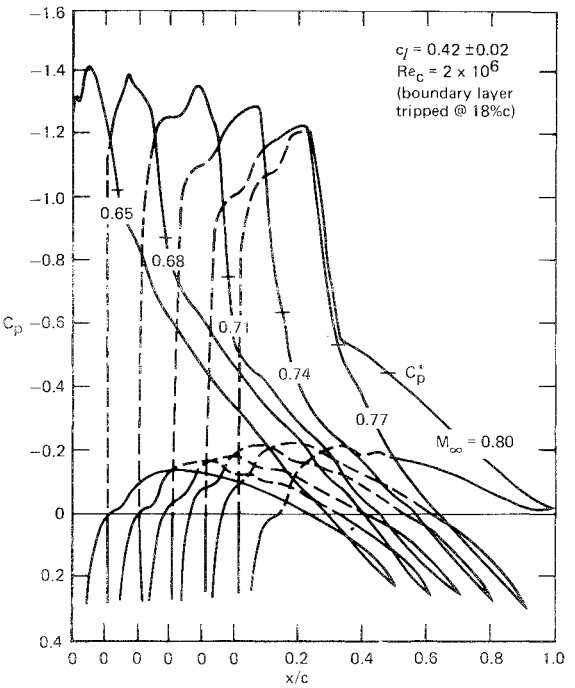

Fig. 4 Pressure distribution on NACA 0012 airfoil as a function of increasing Mach number.

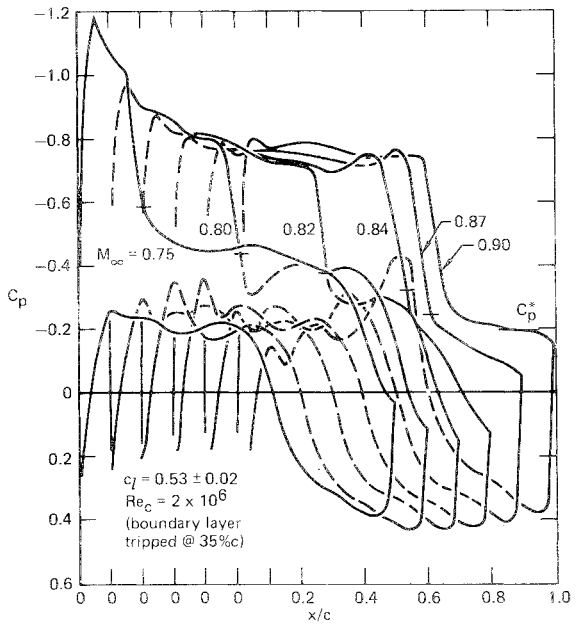

Fig. 3 Development of pressure distribution on supercritical airfoil as Mach number is increased.

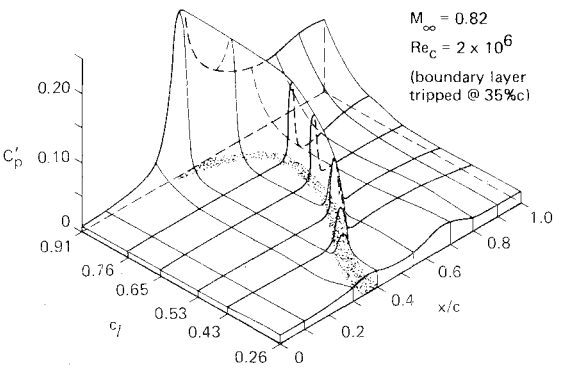

Fig. 5 Evolution with increasing lift coefficient of upper-surface fluctuating pressure distribution on a supercritical airfoil (shaded area indicates location of shock region).

shock-induced separation appears as a local bubble that grows with increasing c_l until it reaches the trailing edge. The evolution with increasing c_l differs from Fig. 4 primarily in the development of greater suction and correspondingly stronger shocks.

The change in sign of ΔC_p over the last 10-20% chord that exists for all C_p distributions except that at the highest M_∞ in Fig. 4 resulted from a minor probe interference problem. In many cases, especially when the shock was well forward on the airfoil, the mechanism holding the shock-position-sensing probe was close enough to the upper surface of the airfoil to alter the flow near the trailing edge. The interference was manifested in two ways: C_p was increased over the aft portion of the upper surface, and the shock location was shifted slightly (usually moved upstream by a few percent chord). This effect was observed with both airfoils.

Several cases, run both with and without the shock probe in place, were compared to evaluate the extent of probe interference, both statically and dynamically. Results of this comparison show that probe interference produced no significant qualitative effect on onset or extent of flow separation, nor on the intensity or spectral content of pressure fluctuations.

Pressure, Lift, and Shock Position Fluctuations

Local surface pressure fluctuations on the supercritical airfoil increase dramatically in intensity with the development of extensive separation, as Fig. 5 indicates. Although the most intense fluctuations are always those associated with the shock wave, heavy buffeting results when the increased fluctuation level caused by flow separation spreads forward to the shock. Figure 6 gives the evolution of the C_p' distribution with increasing M_∞. Although the fluctuating pressures near the trailing edge did intensify at the high Mach numbers, buffeting did not commence, as was indicated by the mean C_p distributions of Fig. 3. The moderately high C_p' levels aft of

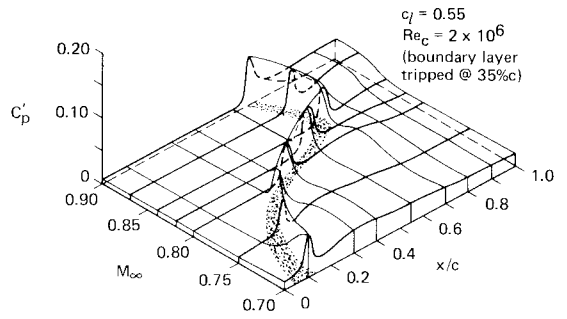

Fig. 6 Chordwise fluctuating pressure distribution for supercritical airfoil: evolution with Mach number variation (shaded area indicates location of shock region).

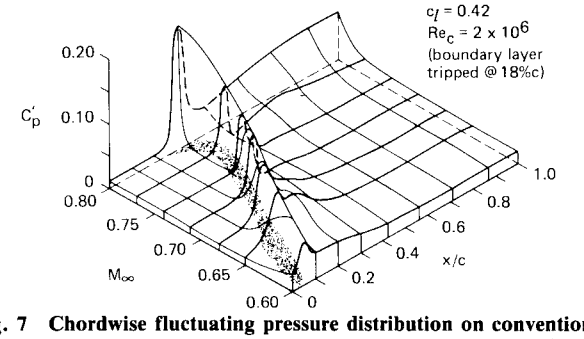

Fig. 7 Chordwise fluctuating pressure distribution on conventional NACA 0012 airfoil: variation with increasing Mach number (shaded area indicates shock region).

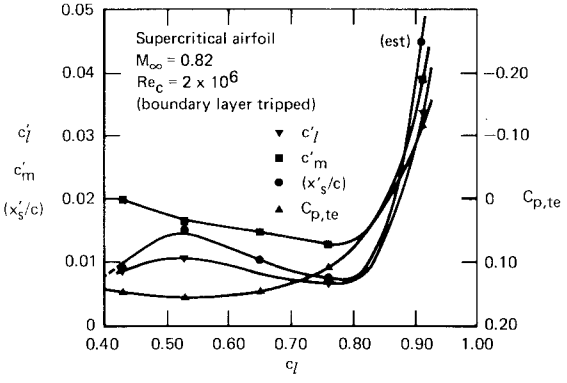

Fig. 8 Lift fluctuations and shock oscillations as a function of increasing static lift on a supercritical airfoil.

the shock at low c_l (Fig. 5) and low M_∞ (Fig. 6) resulted from upstream-propagating shocklets.[5,10]

Fluctuating pressure intensities on the conventional airfoil vary similarly, as Fig. 7 demonstrates. Again, the most intense pressure fluctuations are produced by shock unsteadiness, and significant buffeting develops when separation extends from shock to trailing edge. In this case, though, the rise in C'_p from separation effects first appears just downstream of the shock instead of at the trailing edge, because the separation begins as a bubble (recall Fig. 4). The region of increased C'_p grows toward the trailing edge in direct correspondence with the expansion of the shock-induced separation bubble.

A comparison of several measures of buffet onset and intensity is given in Fig. 8. Divergence of the trailing-edge pressure coefficient is a common indicator of the onset of separation effects, while a rapid increase in airfoil or wing bending moment fluctuation intensity reliably indicates buffet onset.[11] The agreement of these variables suggests that

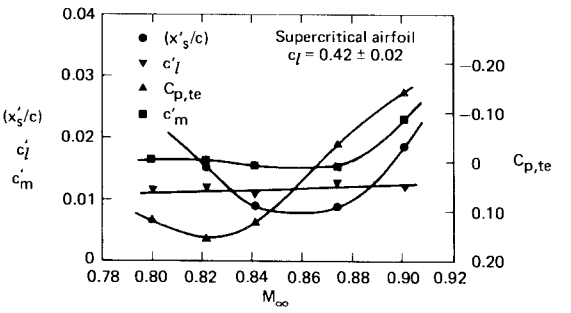

Fig. 9 Variation of supercritical airfoil flowfield unsteadiness with increasing Mach number.

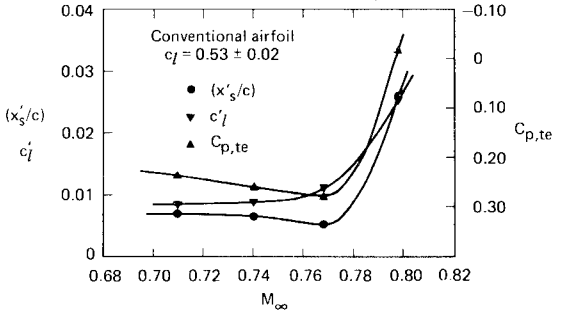

Fig. 10 Influence of Mach number on lift fluctuations and shock oscillations for a conventional (NACA 0012) airfoil.

significant flow separation and buffeting occur simultaneously as lift increases on this supercritical airfoil; this is true of most airfoils. The fact that c'_l, c'_m, and $C_{p,te}$ all vary similarly validates the analog technique employed in approximating the lift fluctuations. Finally, the directly-measured unsteady movements of the upper-surface shock remain at low amplitude until appreciable flow separation occurs. Once separation develops, the coupling of fluctuations of the shock and the separated flow region results in greatly increased amplitudes of shock motion and lift fluctuation.

The relationship of these same variables as Mach number changes is shown in Fig. 9. It is evident that buffeting loads do not develop simultaneously with the $C_{p,te}$ divergence, (which signals the appearance of trailing-edge separation). This buffet-resistant behavior of the supercritical airfoil is beneficial to the transonic performance of a combat aircraft. Recently reported flight-test results obtained by the USAF-NASA TACT supercritical-wing F-111 with wings unswept indeed have shown a constant, high value of buffet-onset lift coefficient throughout the Mach number range, a marked improvement over the standard F-111A with its conventional wing section.[12] The NASA F-8 supercritical-wing airplane has likewise demonstrated a higher-than-cruise value of buffet-onset lift coefficient at all Mach numbers, and has also shown that $C_{p,te}$ divergence is not a valid buffet-onset indicator for the supercritical wing.[13]

The high (x'_s/c) level at the lower Mach numbers in Fig. 9 is associated with the ease of chordwise shock movement resulting from the low pressure gradients existing in the midchord region.

In contrast to the supercritical airfoil, no anomalies appear in the development of separation and buffeting on the NACA 0012 airfoil as M_∞ is increased, as Fig. 10 indicates. All three variables break at approximately the same value of M_∞, providing consistent identification of buffet onset.

The results presented so far have involved only local measurements (e.g., pressure fluctuation intensity at a point) or global features (e.g., lift fluctuations.) Cross correlation was used to establish the spatial and temporal structure of the

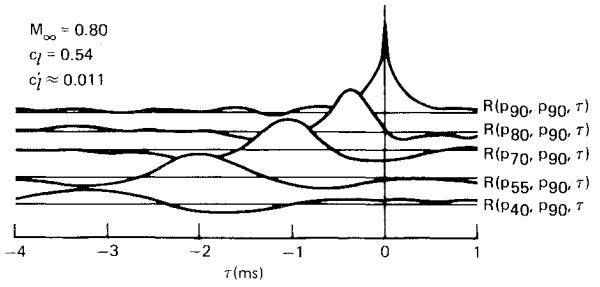

Fig. 11 Disturbance propagation in a supercritical airfoil flowfield: normal case (no separation).

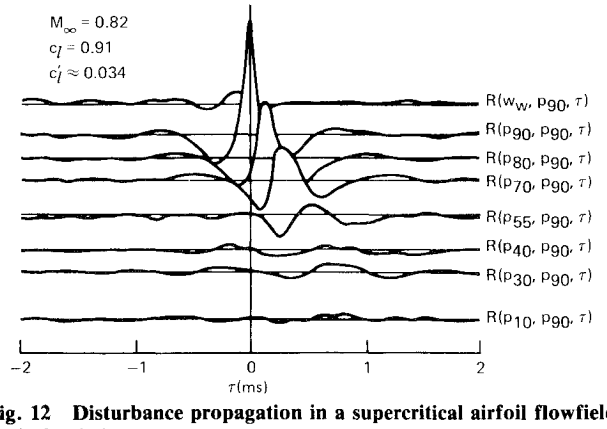

Fig. 12 Disturbance propagation in a supercritical airfoil flowfield: heavy buffeting case.

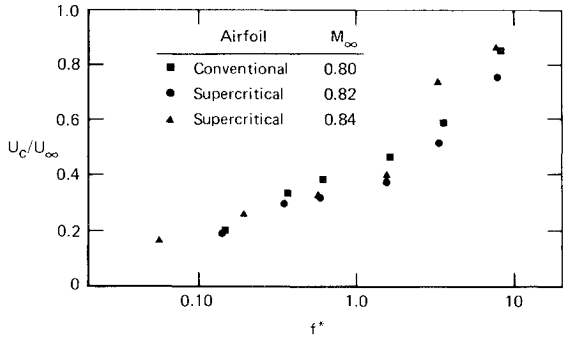

Fig. 13 Pressure fluctuation convection velocities downstream of shock-induced separation.

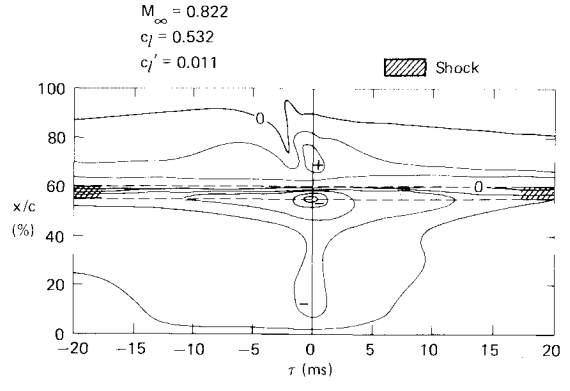

Note: Contours represent increments of 0.1 in cross-correlation coefficient

Fig. 14 Cross correlation of surface pressure and lift fluctuations on a supercritical airfoil in the absence of buffeting.

unsteady pressure fields acting on the airfoils. As Eq. (3) indicates, the cross-correlation coefficient provides a time-averaged measure of how closely one unsteady variable is related to another, taken at a time interval τ later. Variation of τ and the spatial relationship of the two unsteady variables can provide many clues to the characteristics of unsteady flowfields.

Two-Point Pressure Cross Correlations

Two-point pressure cross correlations were used to determine coherence and propagation direction of pressure-fluctuation patterns on the upper surface of the airfoils, especially in the important region of intense pressure fluctuations between the shock and the trailing edge. The transducer nearest the trailing edge (at 90% chord for the supercritical airfoil, 87% chord for the 0012) was used as the reference in each cross correlation. For completely attached flow, the set of cross correlations in Fig. 11 shows that the well-correlated pressure disturbances propagate upstream from the trailing edge to the shock. An average propagation speed can be identified in a cross correlation, using the spatial separation between the measurements and the time delay corresponding to the correlation peak; for the data of Fig. 11, this speed is about 27 m/s (upstream). Since the local flow over this part of the airfoil is nearly sonic, the apparent propagation speed is consistent with the idea of upstream acoustic propagation of pressure disturbances from the trailing-edge/near-wake region. While these data were obtained with the supercritical airfoil, similar results were derived with the conventional section, and the phenomenon is therefore believed to be characteristic of airfoils in transonic flow.

Results differ markedly when the flow is fully separated from the shock to the trailing edge, resulting in heavy buffeting. Such a case for the supercritical airfoil yielded the cross-correlations shown in Fig. 12. The peak time delays are positive instead of negative, indicating that the correlated pressure disturbances are moving downstream. Even the cross correlation between the pressure at 90% chord and the unsteady downwash component of flow velocity just aft of the trailing edge [$R(w_w, p_{90}, \tau)$ in Fig. 12] shows a small peak at a time delay that is consistent with the pressure-pressure cross-correlations, indicating that the coherent pressure disturbances are associated with structures that are being carried downstream with the flow. Comparable results were obtained with the conventional airfoil, leading to the conclusion that this phenomenon, too, is a general one for airfoils undergoing transonic buffeting.

As noted previously, it is possible to derive disturbance-propagation speeds from cross-correlation data. By bandpass filtering the signals before cross-correlation, the frequency dependence of these convection speeds can be established. Convection speed data for three cases of heavy buffeting are plotted in Fig. 13, which shows that the smaller-scale pressure disturbances (associated with the higher frequencies) are convected downstream more rapidly than are the large-scale pressure variations. These results are similar to those obtained from supersonic experiments with step- and ramp-induced separations in two- and three-dimensional flows.[14] Evidently the different pressure-disturbance scales are associated with different levels within the separated shear layer, assuming that the convection speed for a given disturbance corresponds to the local mean flow velocity. Traveling at nearly the free-stream speed, the smallest-scale pressure disturbances apparently arise from the outer edge of the shear layer. This phenomenon contrasts with surface-pressure measurements made beneath attached turbulent boundary layers, which show a slight reduction of convection speed with increasing frequency, in both low-speed[15] and supersonic[14] flows. On the other hand, velocity fluctuation measurements made near the outer edge of an attached turbulent boundary layer have also shown higher convection speeds for higher frequencies.[16] The mechanism by which these small-scale structures near the outer edge of the separated shear layer produce the major

contribution to the high-frequency pressure fluctuations at the wall beneath the separation remains to be defined.

Pressure disturbance propagation appears to be more complex when partial separation exists (e.g., shock-induced separation followed by reattachment). In such cases, the cross-correlations clearly show both up- and downstream propagation of pressure fluctuations, indicating that both the acoustic and convective modes were active. Frequency-resolved cross-correlations show that the higher frequencies ($f^* > \sim 1$) travel downstream with the frequency-dependent speed characteristic of the convective mode, while the lower frequencies show a mixed behavior. This kind of mixed-mode disturbance propagation appears on the 0012 section whenever the flow reattaches, whether or not significant buffeting exists, and also appears on the supercritical airfoil when trailing-edge separation occurs downstream of (rather than at) the shock (e.g., $M_\infty = 0.87$ and 0.90 in Fig. 3).

Pressure/Lift Cross Correlations

To properly characterize the buffeting process, it is necessary to establish which regions of the pressure field are significant contributors to the overall lift force fluctuations; these fluctuations are usually the forcing function in aircraft buffeting. This determination was made through study of cross-correlations between the various fluctuating pressures measured on the airfoil upper surface and the unsteady lift force acting on the airfoil.

The pressure/lift cross correlations are presented in the form of space-time cross-correlation maps. These maps can be interpreted as averaged x-t diagrams of the pressure disturbances that correlate with the unsteady lift. The function plotted is in coefficient form, i.e., the cross-correlation has been normalized by the root-mean-square values of the two correlated variables, as was indicated in Eq. (3). Because of sign conventions on pressure and c_l, a positive pressure change on the upper surface of the airfoil normally corresponds to a reduction in c_l, so that the resulting cross-correlation is negative. The convention on τ for this cross correlation is such that $\tau > 0$ means a delay of the lift force relative to the pressure.

A space-time pressure/lift correlation map corresponding to buffet-free flow about the supercritical airfoil is shown in Fig. 14. This case is included as a reference condition against which other cases will be compared. The shock region indicated in Fig. 14 is simply the pressure-rise region of the C_p distribution. The low-level c_l fluctuations arise mainly from pressure fluctuations in the vicinity of the shock, which is undergoing moderate-amplitude chordwise excursions ($M_\infty = 0.82$ point in Fig. 9). The correlated pressure variations change phase across the shock, so that the unsteady pressures up- and downstream of the shock tend to cancel each other. Finally, the distortion of isocorrelation contours near the trailing edge at slightly negative τ is associated with upstream-propagating pressure disturbances; this distortion would be more pronounced if higher frequencies had been included in computing the cross-correlation (only frequencies below 1 kHz were involved).

The cross-correlation map that represents a case of heavy buffeting at high lift ($M_\infty = 0.82$, $c_l = 0.91$) is different. As Fig. 15 shows, the strongest correlation again occurs in the vicinity of the unsteady shock (which is also the location of the most intense pressure fluctuations, Fig. 5), but the magnitude of the correlation has increased from the buffet-free case. A strong correlation of opposite sign near the trailing edge (another region of high pressure-fluctuation intensity) seems to be associated with the previous half-cycle of pressure fluctuation at the shock, and indicates that the trailing-edge flow is a central element in the buffeting process. The time-dependence of the boundary between the regions of positive and negative correlation suggests that pitching moment fluctuations may accompany the lift unsteadiness. Since they are not the result of any coupling between unsteady aerodynamics and airfoil motion, these pitching moment fluctuations differ from those associated with the torsional buffet response sometimes exhibited by finite wings.[4,17] Changes in the location and/or strength of the shock in turn affect the flow separation, and the convection of such changes is indicated by the sweep of the correlation contours toward the trailing edge with increasing τ. Other noteworthy features of the correlation map in Fig. 15 are the low correlation level on the forward part of the airfoil and the slight periodicity (one cycle identifiable on either side of $\tau = 0$).

The next three pressure/lift cross-correlation maps were obtained with the conventional NACA 0012 airfoil. The first of these, presented in Fig. 16, represents the airfoil in a buffet-free condition ($M_\infty = 0.68$, $c_l = 0.42$). As with the supercritical airfoil, the unsteady lift that does exist is

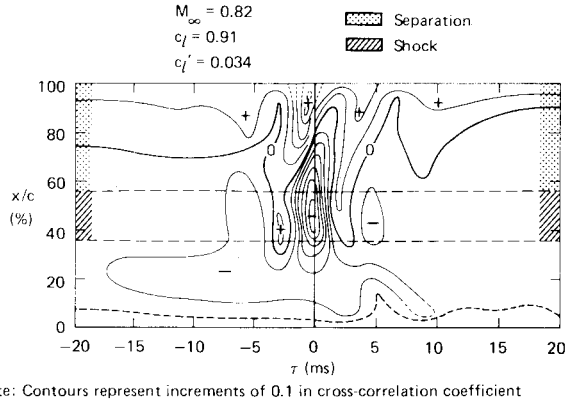

Note: Contours represent increments of 0.1 in cross-correlation coefficient

Fig. 15 Cross correlation of surface pressure and lift fluctuations on a supercritical airfoil in high-lift buffeting.

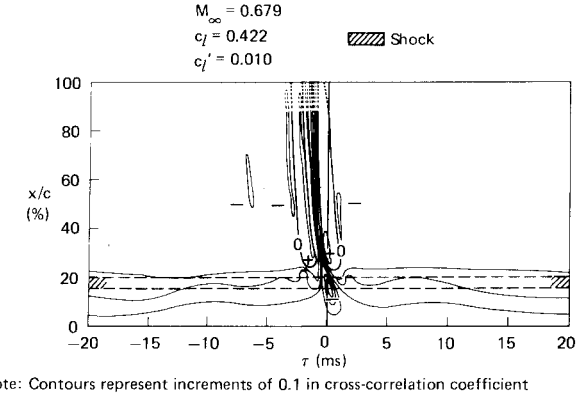

Note: Contours represent increments of 0.1 in cross-correlation coefficient

Fig. 16 Cross correlation of surface pressure and lift fluctuations on a conventional airfoil with no buffeting.

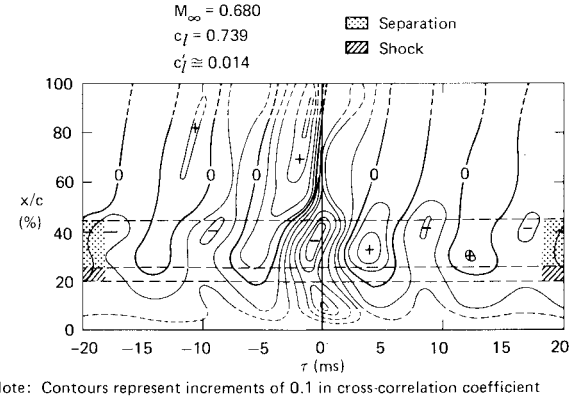

Note: Contours represent increments of 0.1 in cross-correlation coefficient

Fig. 17 Cross correlation of pressure and lift fluctuations on a conventional airfoil at high lift.

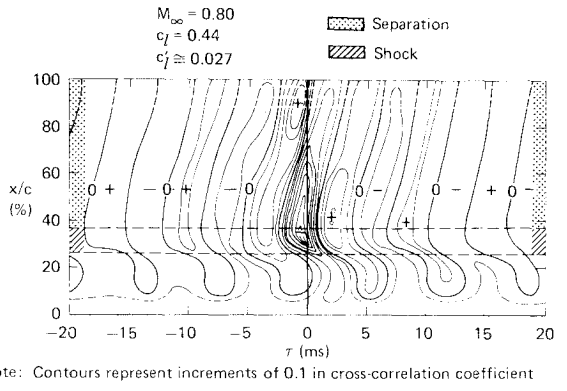

Fig. 18 Cross correlation of local surface pressure and lift fluctuations on a conventional airfoil in high-Mach-number buffeting.

produced mainly by pressure fluctuations near the shock. However, in this case the pressure fluctuations clearly originate at (or aft of) the trailing edge and propagate forward until they affect the shock.

At the highest lift measured ($c_l = 0.74$ at $M_\infty = 0.68$), the 0012 airfoil presents an interesting case of incipient buffeting (Fig. 17). The flow remains attached at the trailing edge for this condition, and there is a large shock-induced separation bubble on the airfoil. The strongest pressure/lift correlation appears to be more closely associated with the separation bubble than with the shock. Because the flow reattaches, the contours of strong correlation do not stretch toward the trailing edge as prominently as they do when the flow is fully separated. The pronounced positive correlation at the trailing edge again appears to result from the prior half-cycle of lift and pressure fluctuation. The greatest positive correlation for $\tau > 0$ occurs not near the trailing edge, but under the separation bubble. As is true for the supercritical airfoil, the time-dependent boundary between the positive and negative correlation zones may be an indication that pitching moment fluctuations exist. One result peculiar to this map is the substantial negative pressure/lift correlation near the leading edge of the airfoil (where fluctuation intensities were low).

The pronounced periodicity of the pressure/lift cross-correlation map in Fig. 17 was characteristic of the 0012 airfoil. Heavy buffeting of this airfoil, which occurred at $M_\infty = 0.80$, $c_l = 0.44$, resulted in similarly strong periodicity, as Fig. 18 shows. Comparison of Figs. 17 and 18 reveals that the frequency indicated by the cross-correlation map is not the same in the two cases. There is no connection between this periodicity and spanwise bending vibrations of the airfoil model. The frequency appearing in these cross-correlation maps varies according to flow conditions and is always greater than the spanwise bending mode frequency.

Many of the features of the pressure/lift cross-correlation for the conventional 0012 airfoil in heavy buffeting are similar to those of the supercritical section, suggesting that these features are common to transonic airfoil flows in general. As with the supercritical section, the strongest correlation is associated with movement of the shock wave and the resulting shock-induced separation, and a significant correlation of opposite sign again appears near the trailing edge. The manner in which the correlation contours sweep toward the trailing edge with increasing τ again identifies this phenomenon with a shear-layer convection process. The fore and aft phase reversal of the correlation in Fig. 18 is similar to that shown by the supercritical airfoil, although the negative peak is stronger and the positive peak is weaker for the conventional section. This difference in relative strengths of positive and negative correlation peaks implies that pitching moment fluctuations may be less important, relative to lift fluctuations, for the conventional airfoil than they are for the supercritical section. Although slight correlation does exist upstream of the shock, with the contours skewed by the low speed associated with disturbance propagation around the supersonic zone, the contribution of pressure fluctuations in this area to the unsteady lift is insignificant, as it is with the supercritical airfoil.

The one striking difference between the pressure/lift cross-correlation maps for the two airfoils in buffeting is the almost complete absence of periodicity in the supercritical airfoil correlations, compared to the pronounced periodicity evident in the correlations for the conventional NACA 0012 section. The greater periodicity seen in the lift and pressure fluctuations for the conventional airfoil in buffeting results from closer coupling of three elements of the unsteady transonic flowfield for that airfoil: the shock, the separated flow, and lift. As discussed earlier, the type of flow separation is different for the two airfoils. The curvature of the upper surface that results from the rearward camber of the supercritical airfoil promotes a trailing-edge separation that develops well before buffet onset (recall Fig. 9). Even when separation reaches the shock so that buffeting exists, pressure disturbances that arise in the shock-induced separation region and are subsequently convected downstream lose coherence before reaching the trailing edge (Fig. 15); consequently these pressure disturbances do not have an organized effect on circulation adjustment (which corresponds to lift variation) at the trailing edge. On the conventional 0012 airfoil, flow separation begins as a shock-induced separation bubble that grows until it reaches the trailing edge. In this case, convected pressure fluctuations remain coherent all the way to the trailing edge, and therefore have a more profound effect on circulation changes that occur there.

Shock-displacement/lift-fluctuation cross correlations revealed that coupling between shock motion and unsteady lift during buffeting is also greater for the conventional airfoil. The magnitude of the peak correlation is higher and the periodicity is more pronounced for the 0012 airfoil, consequences of the differences in chordwise pressure gradients on the upper surface of the two airfoils. The steep chordwise gradients on the 0012 section mean that small displacements of the shock correspond to appreciable lift changes and substantial variations in shock strength. Because of the flat upper surface, the supercritical airfoil has a correspondingly flat upper-surface pressure distribution that allows the shock to move chordwise with comparatively little change in lift, and almost no change in strength.

Conclusions

Experimental study of unsteady pressure fields that are responsible for transonic airfoil buffeting has provided new insight into the structure of the associated unsteady flow mechanisms.

For both a conventional NACA 0012 airfoil and a Whitcomb-type supercritical section, the surface-pressure and lift-force fluctuations are associated primarily with the upper-surface shock and the region of separated flow between the shock and the trailing edge. On the aft-cambered supercritical airfoil, separation and the corresponding increase of C_p' always begin at the trailing edge; for the conventional 0012 airfoil, the C_p' rise first appears beneath a shock-induced separation bubble that grows toward the trailing edge with increasing c_l or M_∞.

Between the upper-surface shock and the trailing edge (a region of intense pressure fluctuations), pressure disturbances on both airfoils are propagated upstream acoustically when the flow is attached, but are convected downstream in fully separated flow. In the latter situation only, the pressure fluctuation convection speed is strongly frequency-dependent, with the higher frequency (smaller scale) disturbances moving more rapidly.

Cross correlations relating local surface pressures to lift fluctuations were helpful in defining the spatial and temporal structure of the buffet-producing unsteady pressure field. For

both airfoils, pressure fluctuations at the trailing edge are out of phase with those near the shock, in terms of contribution to unsteady lift. This suggests that pitching moment fluctuations might also be present in airfoil buffeting.

The supercritical airfoil differs from the conventional section in two aspects: 1) a reduced tendency to develop buffeting fluctuations as flow separation effects grow with increasing M_∞ and 2) less-periodic lift and pressure fluctuations once significant buffeting does develop. These differences are attributed to reduced coupling of lift, shock location, and flow separation fluctuations for the supercritical airfoil, which results from the characteristic flat-topped, aft-cambered shape of the supercritical section.

Acknowledgment

This research was conducted under the McDonnell Douglas Independent Research and Development Program in cooperation with the NASA Ames Research Center.

References

[1] *Unsteady Airloads in Separated and Transonic Flow, Proceedings of 44th Meeting of AGARD Structures and Materials Panel,* AGARD-CP-226, Lisbon, Portugal, April 1977.

[2] *Aircraft Stalling and Buffeting,* AGARD-LS-74, presented at the von Kármán Institute, Brussels, and NASA Ames Research Center, Calif., March 1975.

[3] Mullans, R.E. and Lemley, C.E., "Buffet Dynamic Loads During Transonic Maneuvers," McDonnell Aircraft Co., AFFDL-TR-72-46, 1972.

[4] Cunningham, A.M. Jr. and Benepe, D. B. Sr., "Prediction of Transonic Aircraft Buffet Response," *Proceedings of the 44th Meeting of AGARD Structures and Materials Panel,* AGARD-CP-226, Lisbon, Portugal, April 1977.

[5] Roos, F.W., "Surface Pressure and Wake Flow Fluctuations in a Supercritical Airfoil Flowfield," AIAA Paper 75-66, Pasadena, Calif., Jan. 1975.

[6] Hurley, F.X., Spaid, F.W., Roos, F.W., Stivers, L.S. Jr., and Bandettini, A., "Supercritical Airfoil Flowfield Measurements," *Journal of Aircraft,* Vol. 12, Sept. 1975, pp. 737-744.

[7] Whitcomb, R.T., "Review of NASA Supercritical Airfoils," ICAS Paper No. 74-10, presented at the 9th Congress of the International Council of Aeronautical Sciences, Haifa, Israel, Aug. 1974.

[8] Roos, F.W., "Hot-Film Probe Technique for Monitoring Shock-Wave Oscillations," *Journal of Aircraft,* Vol. 16, Dec. 1979, pp. 871-875.

[9] Bendat, J.S. and Piersol, A.G., *Random Data: Analysis and Measurement Procedures,* Wiley, N.Y., 1971.

[10] Roos, F.W. and Riddle, D.W., "Measurements of Surface-Pressure and Wake-Flow Fluctuations in the Flow Field of a Whitcomb Supercritical Airfoil," NASA TN D-8443, Aug. 1977.

[11] Huston, W.B., "A Study of the Correlation Between Flight and Wind-Tunnel Buffet Loads," AGARD Rept. 111, 1957.

[12] Monaghan, R.C., "Flight-Measured Buffet Characteristics of a Supercritical Wing and a Conventional Wing on a Variable-Sweep Airplane," NASA TP-1244, May 1978.

[13] DeAngelis, V.M. and Monaghan, R.C., "Buffet Characteristics of the F-8 Supercritical Wing Airplane," NASA TM 56049, Sept. 1977.

[14] Coe, C.F., Chyu, W.J., and Dods, J.B. Jr., "Pressure Fluctuations Underlying Attached and Separated Supersonic Turbulent Boundary Layers and Shock Waves," AIAA Paper 73-996, Seattle, Wash., Oct. 1973.

[15] Willmarth, W.W., "Pressure Fluctuations Beneath Turbulent Boundary Layers," *Annual Review of Fluid Mechanics,* Vol. 7, 1975, pp. 13-38.

[16] Cliff, W.C. and Sandborn, V.A., "Measurements and a Model for Convective Velocities in the Turbulent Boundary Layer," NASA TN D-7416, Oct. 1973.

[17] Moss, G. F. and Pierce, D., "The Dynamic Response of Wings in Torsion at High Subsonic Speeds," *Proceedings of 44th Meeting of AGARD Structures and Materials Panel,* AGARD-CP-226, Lisbon, Portugal, April 1977.